Supplementary information

One-step synthesis of hollow spherical Co/Ni hydroxides as multifunctional polysulfide mediators to steer sulfur redox kinetics for high performance lithium-sulfur batteries

Zhen Li[a, b#,*], Man Yang[a, c#], Qing Li[a, b#], Xianghan Cheng[a, d], Fengting Geng[a, d], Yuye Wang[a], Xiaoli Wang[a], Dashuai Zhang[a], Yongzheng Zhang[a], Xiuling Zhang[a], Zhongmin Liu[a], Xuliang Pang[a], Longlong Geng[a, b*]

[a] *College of Chemistry and Chemical Engineering, Dezhou University, Dezhou 253023, China.*

[b] *Shandong Provincial Key Laboratory of Monocrystalline Silicon Semiconductor Materials and Technology, Dezhou University, Dezhou 253023, China.*

[c] *School of Chemical Engineering and Technology, North University of China, Taiyuan 030051, China.*

[d] *School of Chemistry and Chemical Engineering, Shandong University of Technology, Zibo 255000, China.*

[#] *These authors contributed equally to this work.*

* *Corresponding author: lizhendiyi@163.com (Zhen Li); llgeng@126.com(Longlong Geng)*

1. Material characterizations

The crystallinity of the materials was characterized a BRUKER D2 PHASER X-Ray Diffractometer with Cu Kα radiation (λ = 1.5418 Å). The micro-structure of the materials was monitored by using scanning electron microscope quipped with an energy dispersive X-ray spectrometer (SEM-EDX, Hitachi S4800) and transmission electron microscope (TEM, Hitachi H-800 TEM at 200 kV). Electron paramagnetic resonance (EPR, Bruker A300) was adopted to study the vacancies in the materials. The porous feature of the materials was proofed by the N_2 adsorption and desorption technique (Micromeritics ASAP 2020). X-ray photoelectron spectroscopy (XPS) was collected on a Thermo ESCALAB 250XI machine equipped with an Al Kα X-ray source. Thermal gravity analysis (TGA, Thermo Scientific Nicolet iS50) was used to

investigate the thermal behaviors of the materials. The Ni and Co K-edge X-ray absorption fine structure (XAFS) spectra were collected at BL11B beamline of Shanghai Synchrotron Radiation Facility, China. The acquired EXAFS data were analyzed by adopting a standard procedure through the ATHENA module in the IFEFFIT software packages [1, 2]. The Wavelet transform (WT) of k^2-weighted EXAFS spectra (WT-EXAFS) was performed through the Hama software.

2. Electrochemical measurements

Li-S Cell Assembly and Measurements. The active materials, Super P, and binder (polyvinylidene fluoride, PVDF) in a weight ratio of 7:2:1 was dispersed into N-methyl pyrrolidone (NMP) to form a stable slurry. The working electrode was prepared by coating the slurry of onto a round-shaped Al foil (1.1 cm^2). The electrochemical performance of the as-fabricated working electrodes was examined using CR2032 coin-type cells. 1 M lithium bis(trifluoro-methane-sulfonyl) imide (LiTFSI) and 0.1 M of $LiNO_3$ in a mixture of dioxolane (DOL) and 1,2-dimethoxy ethane (DME) with a volume ratio of 1: 1 was used as the electrolyte. The loading density of the active material is about 1.0 mg cm^{-2} and the electrolyte/sulfur ratio (E/S) is 15 μL mg^{-1} for each cell, which is a popular parameter for coin-type Li-S cells in the lab.[3-5] Lithium foil was used as both the counter electrode and the reference electrode. The loading density of Li foil is about 21 mg cm^{-2}. The ratio between the theoretical capacities of the negative electrode and the positive electrode (N/P) is calculated to be 50.7, which is comparable to the previous reported value for the coin-type Li-S cells in the lab (N/P = 61.2).[6] Celgard 2400 membranes were used as separators. The electrochemical performance of the working electrodes was tested by using a battery test system (NEWARE CT-4008Tn). Li-S cells with a higher sulfur loading density (5.2 mg cm^{-2}, corresponding to N/P = 9.7) and lean electrolyte content (E/S = 4 μL mg^{-1}) were also assembled. Cells were galvanostatically cycled within the potential window of 1.7-2.8 V vs. Li/Li^+ and activation treatment at a low current of 0.05 C was conducted before the cycling test. Electrochemical impedance spectra (EIS) were collected for the cells at an open potential over the frequency range from 100 kHz to

0.01 Hz on an electrochemical workstation (Shanghai Chen Hua, CHI660E). Cyclic voltammetry (CV) was performed on the cathodes at various scan rate ranging from 0.1 to 0.4 mV s^{-1} within the potential window of 1.7–2.8 V.

Preparation of Li_2S_6 and Li_2S_8 Solutions. Sulfur and Li_2S in different mass ratios (1:5 for Li_2S_6 and 1:7 for Li_2S_8) were added into a mixed solvent of DME and DOL (1:1, v/v) and the mixture was vigorously stirred for 12 h until a dark yellow solution was formed.

Li_2S_6 adsorption test of the materials. 10 mg of the materials were dispersed into 3.0 mL of Li_2S_6 solution (0.05 M) and stirred for 4 h. The UV-vis spectra (Shimadzu, UV-2700) of the supernatant solution was checked to evaluate the adsorption performance of the materials.

Symmetric cell fabrication and test: Bare H-Co and H-Ni, as well as the bimetallic H-Co_xNi_{1-x} were used as the active materials. The working electrodes for symmetric cells were fabricated in the same way as electrodes for LSBs. Two pieces of the same electrodes were used as identical working and counter electrodes. Li_2S_6 solution (0.5 M) containing 1 M LiTFSI in DOL/DME (v/v, 1/1) was used as the electrolyte. The symmetric cells were assembled in the same way with that of Li-S coin-type cells. CV measurements were performed at a scan rate of 5 mV/s.

Measurement of nucleation of Li_2S. The nucleation of Li_2S were tested in CR2032 coin-type cells. The working electrodes were prepared by dispersing the host materials in absolute ethyl alcohol to form a slurry which was subsequently coated on a carbon paper disk (1.1 cm^2) and dried at 60 ºC overnight. Li foil served as the counter electrode, 20 μL of 0.25 M Li_2S_8 solution containing 1.0 M LiTFSI was used as catholyte, and 20 μL of 1.0 m LiTFSI in DOL/DME (v/v=1:1) solution as anolyte. The cells were firstly discharged to 2.19 V at a constant current of 0.112 mA to reduce the higher-order LiPSs to Li_2S_4 and then further held at 2.05 V until the current decreased to 0.01 mA to monitor the Li_2S nucleation. Similar experimental procedure has also been adopted in the previous reports.[3, 5, 7]

3. DFT calculations

The monolayered model was constructed based on the previous reports [8-10]. Dmol3 module in the Material Studio software package was used for DFT calculations. The generalized gradient approximation (GGA) with the Perdew-Burke-Ernzerhof (PBE) functional and the double numerical plus d-functions (DNP) basis set were used in geometry optimization. A vacuum layer of 15 Å was established along the planer direction of the materials. The convergence criteria of the SCF calculation were set to 10^{-5} eV. For the geometry optimization of the system, the energy, force and displacement convergence criterions were set as 2×10^{-5} Ha, 4×10^{-3} Ha and 5×10^{-3} Å, respectively. The adsorption energy of LiPSs on the surface of the host materials was defined as following:

$$E_b = E(Li_2S_n/host) - E(Li_2S_n) - E(host)$$

where E_b was the electronic adsorption energy, $E(Li_2S_n/host)$ is the electronic energy of the slab and Li_2S_x complex, E(host) and $E(Li_2S_n)$ represent the electronic energy of the standing alone host material and Li_2S_x molecules, respectively.

4. Supplementary data

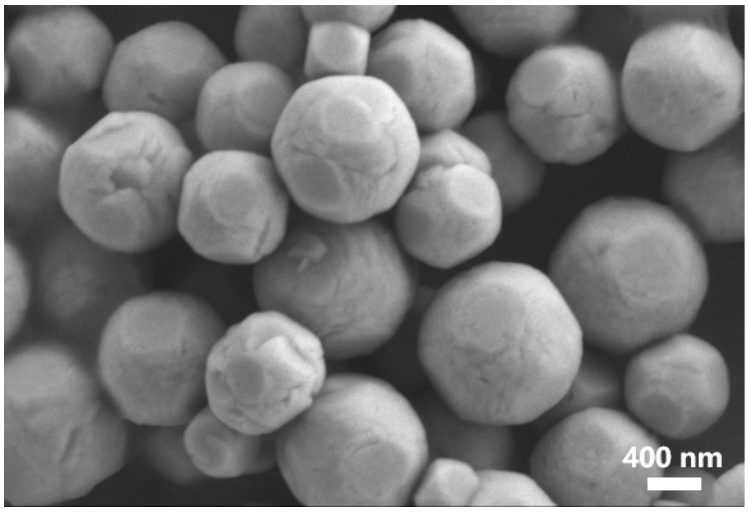

Fig. S1 SEM image of Cu_2O spheres

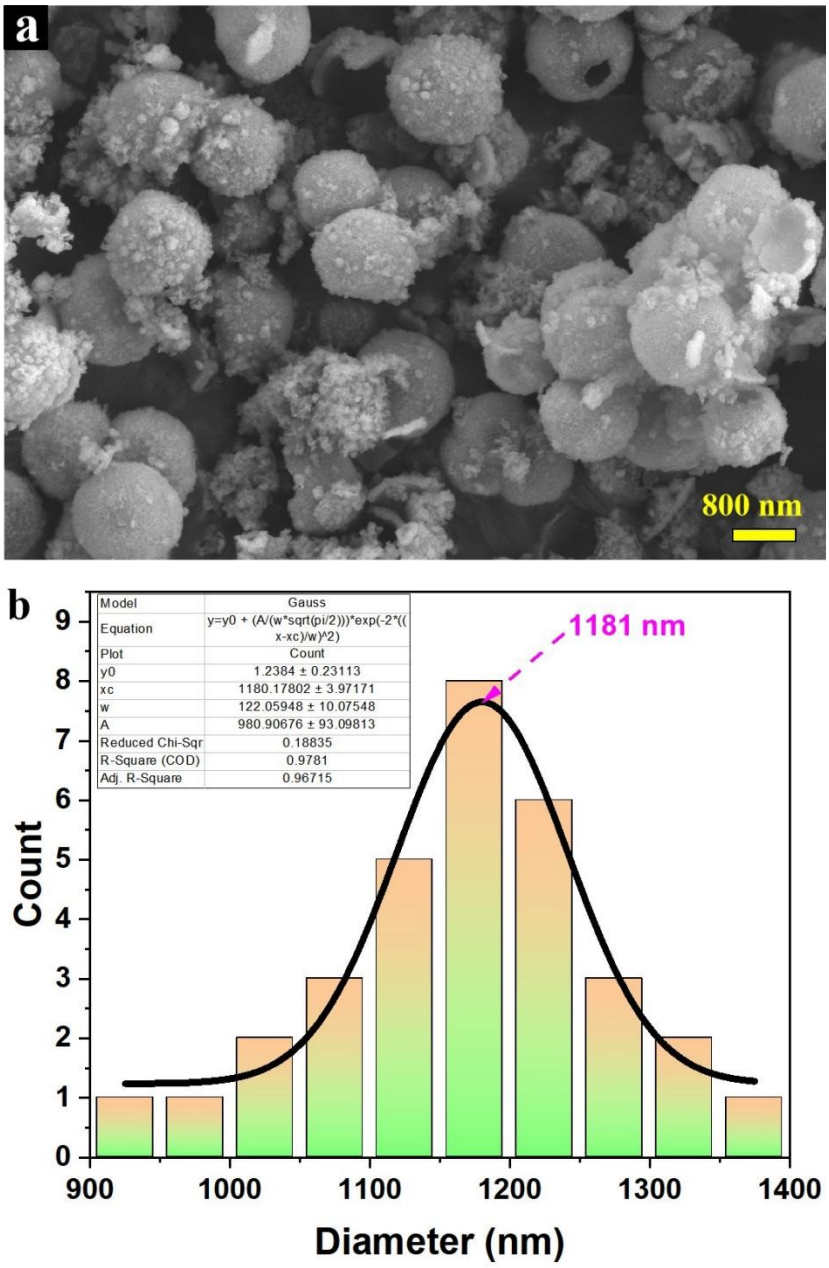

Fig. S2 SEM image of H-$Co_{0.4}Ni_{0.6}$ (a) and the corresponding particle size distribution curve (b).

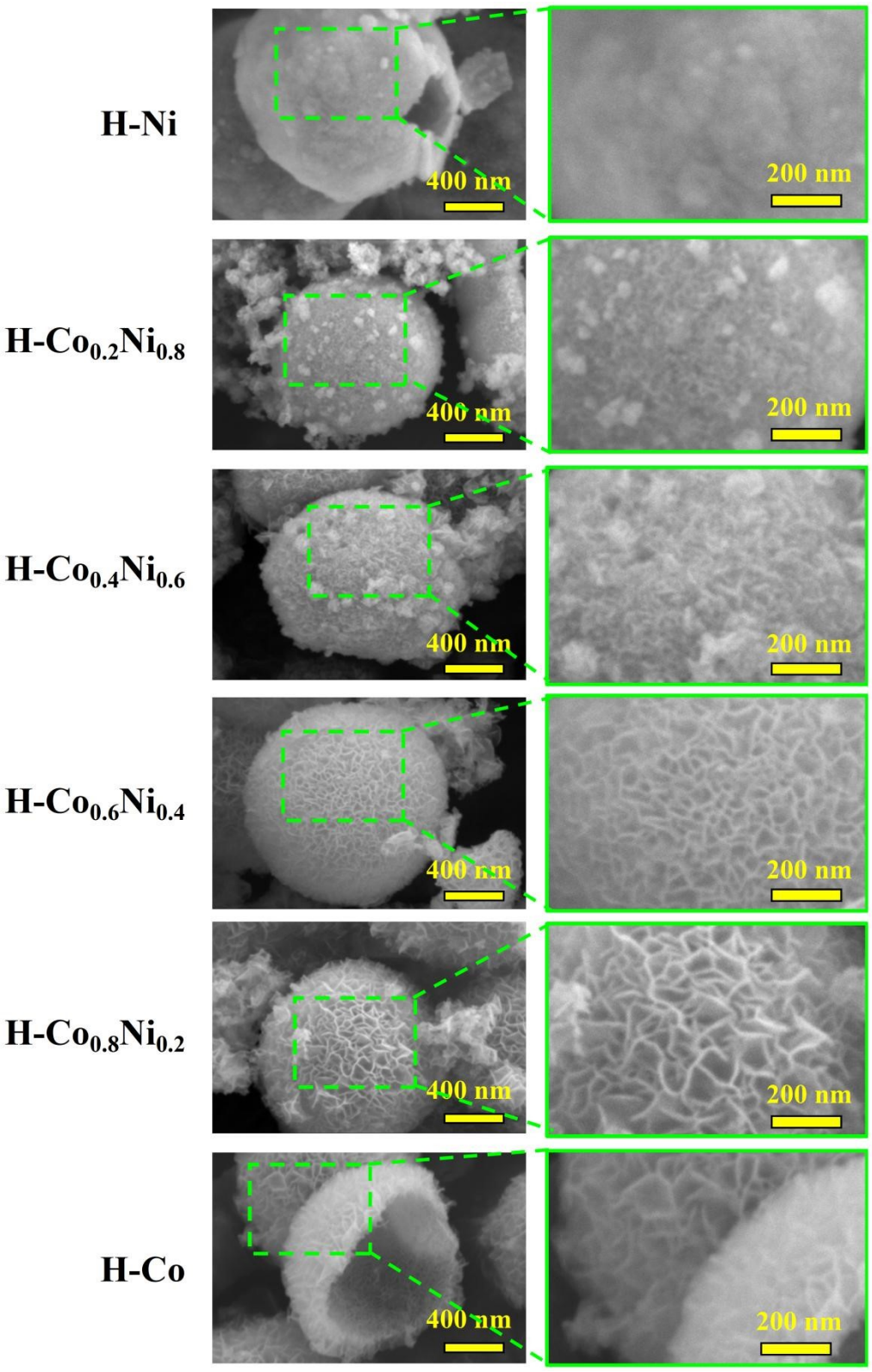

Fig. S3 SEM images of the spherical H-Co_xNi_{1-x} materials at different magnifications.

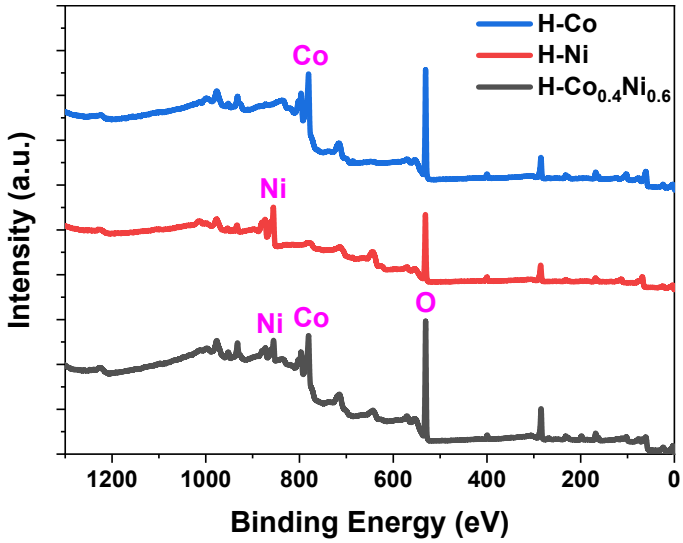

Fig. S4 XPS Survey spectra of the materials

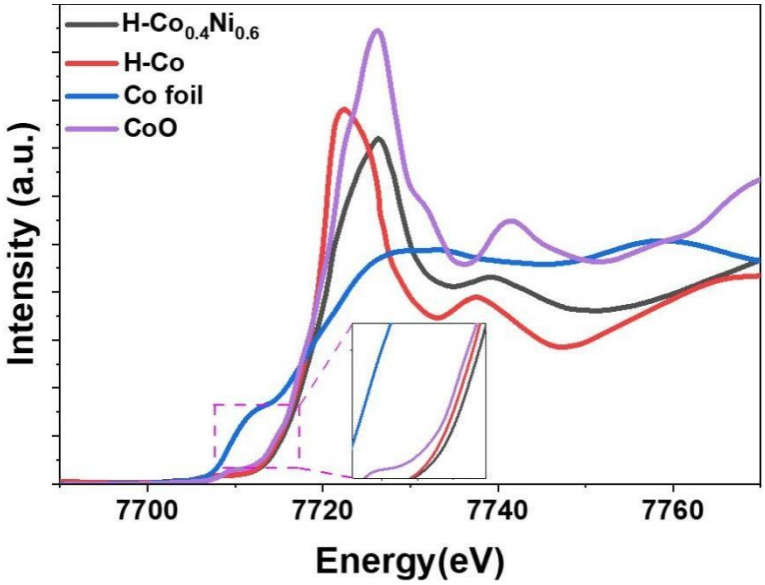

Fig. S5 X-ray absorption near edge structure (XANES) data of the materials

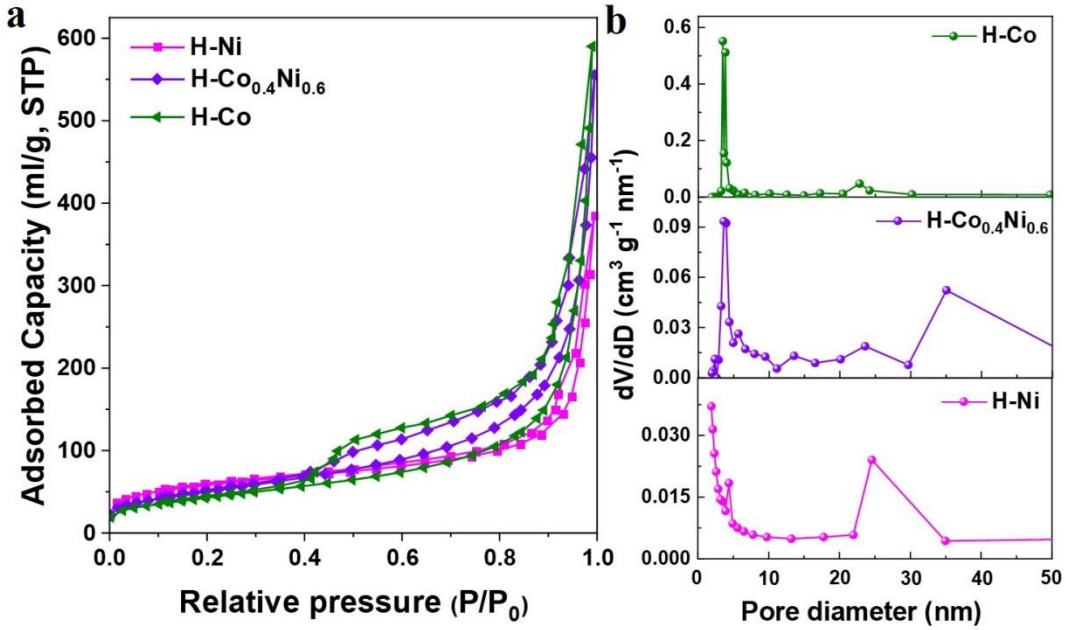

Fig. S6 N_2 adsorption–desorption isotherms (a) and their corresponding pore size distribution curves based on the desorption curves of H-Co, H-Ni and H-$Co_{0.4}Ni_{0.6}$.

Table S1 Summary of the analysis for N_2 adsorption–desorption date of the materials

Samples	BET surface area (m^2/g)	Pore size (nm)	Pore volume (cm^3/g)
H-Co	158.08	3.45	0.96
H-$Co_{0.4}Ni_{0.6}$	185.34	3.60	0.83
H-Ni	210.12	1.90	0.53

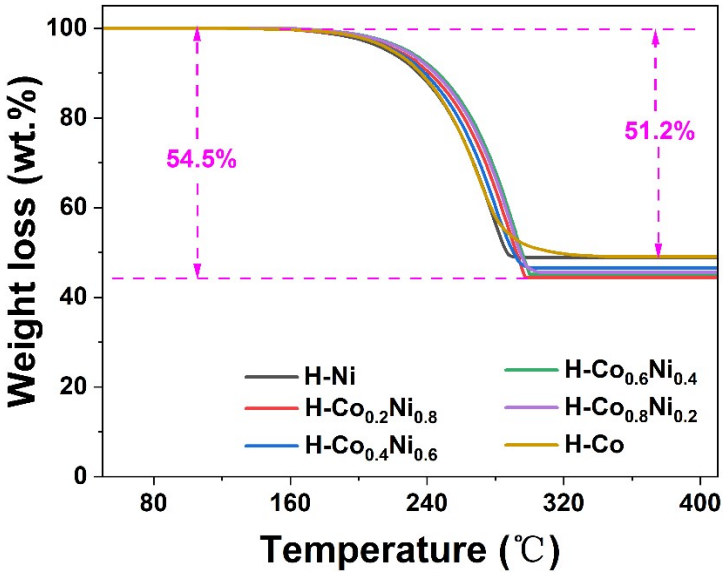

Fig. S7 TGA curves of H-Co_xNi_{1-x}@S composites

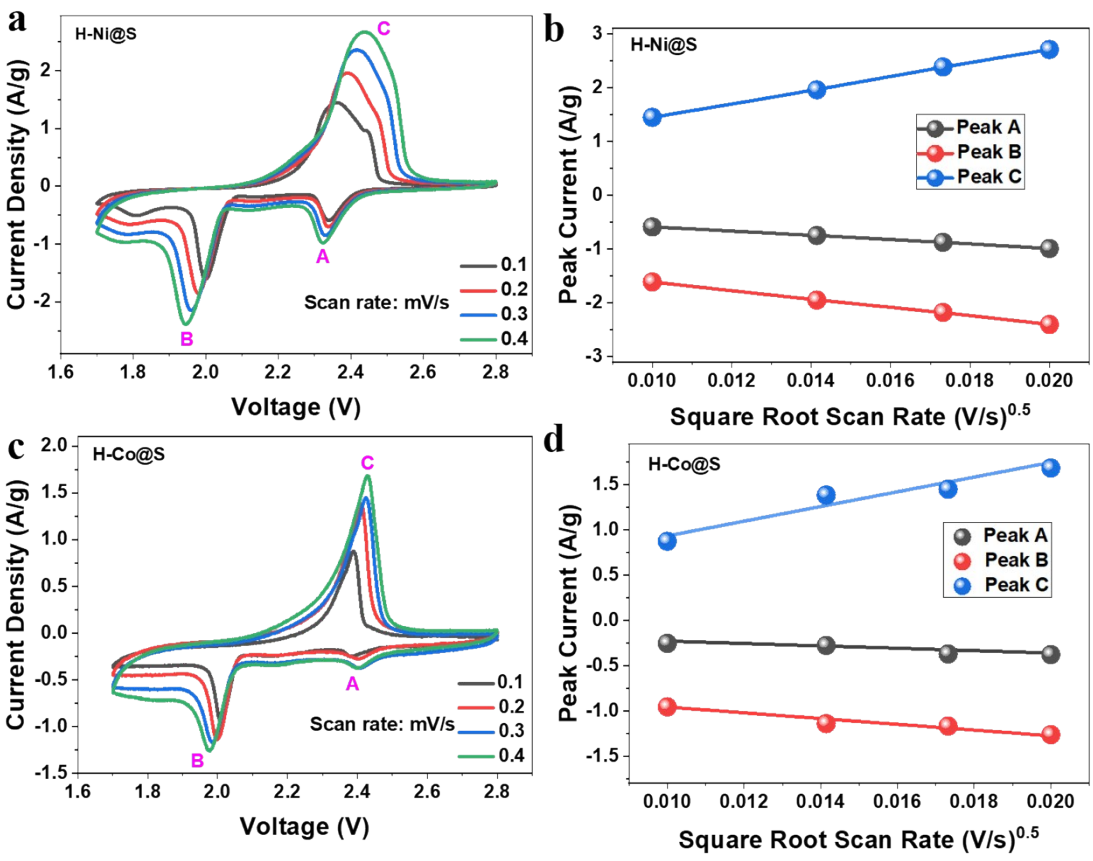

Fig. S8 (a and c) CV curves of H-Ni@S and H-Co@S electrodes at various scanning rates; (b and d) plot of CV peak current versus the square root of scan rates for H-Ni@S and H-Co@S electrodes.

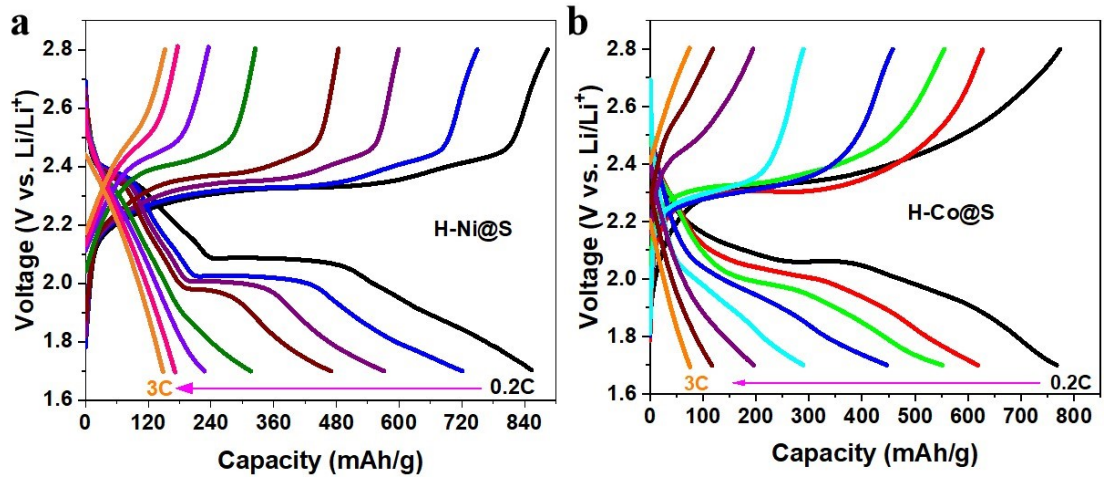

Fig. S9 Charge and discharge curves of H-Ni@S (a) and H-Co@S (b) cathodes at various current rates.

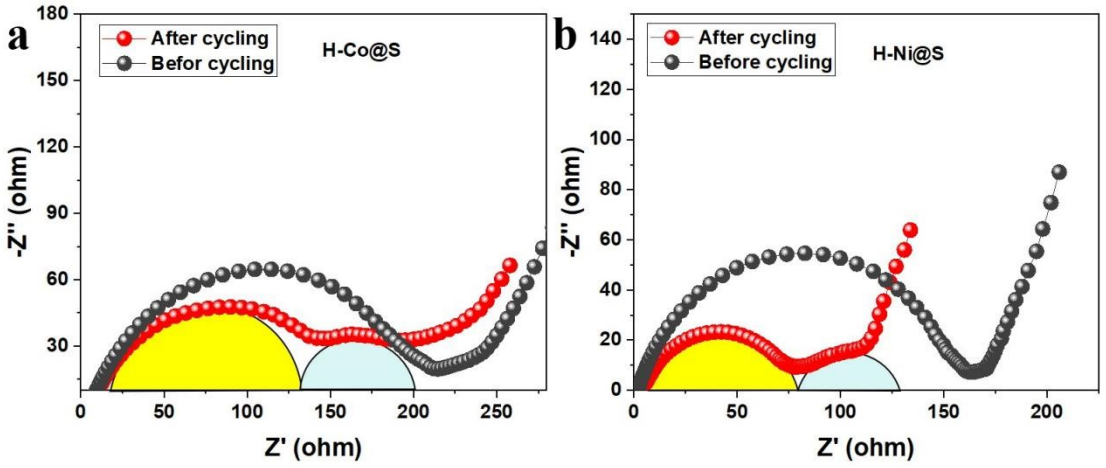

Fig. S10 EIS spectra of the H-Co@S and H-Ni@S electrodes at different cycling states.

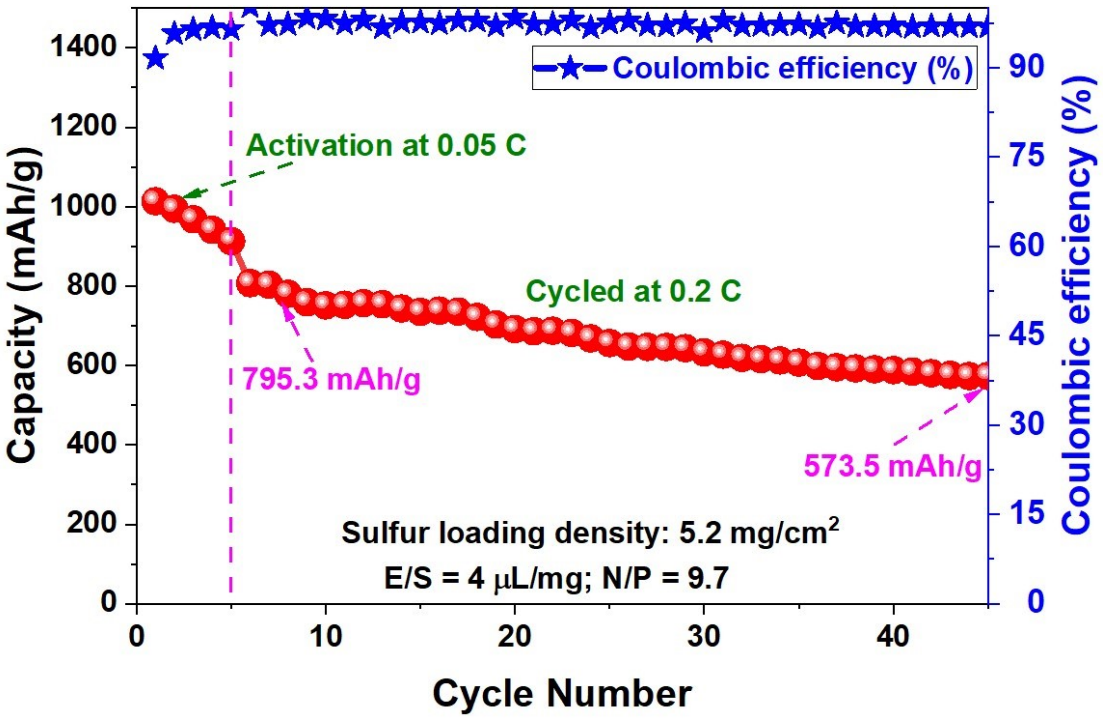

Fig. S11 Cycling stability test of the H-$Co_{0.4}Ni_{0.6}$@S-based cell with a higher sulfur loading density and lean electrolyte content.

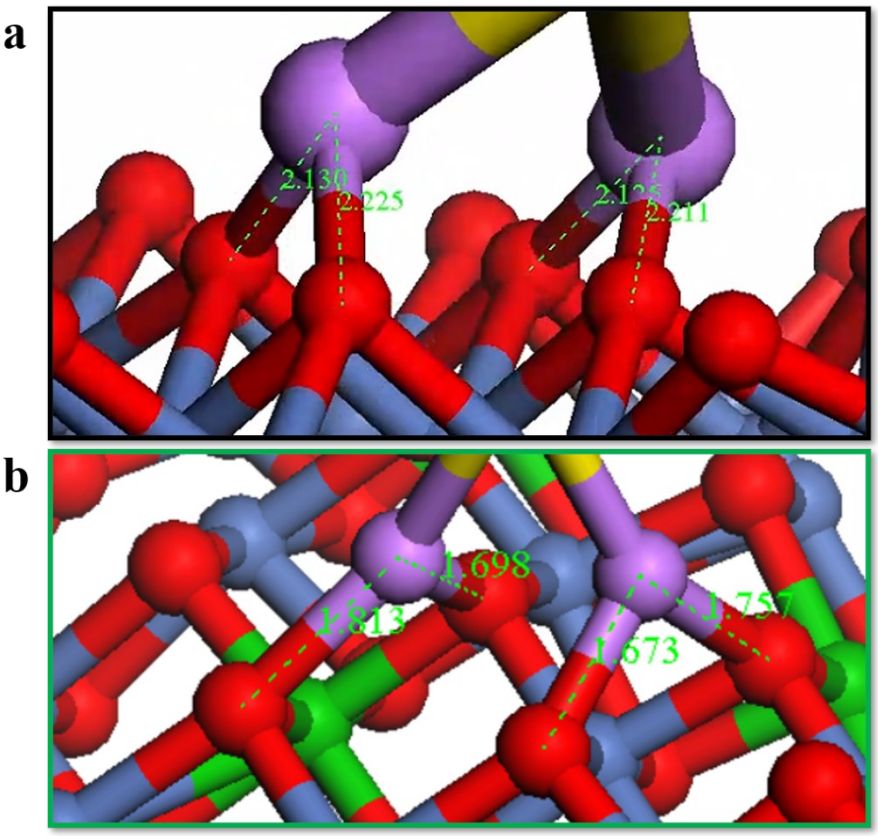

Fig. S12 Comparison of Li-O bond distance between Li_2S/H-Ni (a) and Li_2S/H-$Co_{0.4}Ni_{0.6}$ (b) systems.

References:

1. Matthew, N., IFEFFIT: interactive XAFS analysis and FEFF fitting. *Journal of synchrotron radiation* **2001,** *8,* (2), 322-324.

2. Ravel, B.; Newville, M., ATHENA,ARTEMIS,HEPHAESTUS: data analysis for X-ray absorption spectroscopy usingIFEFFIT. *Journal of Synchrotron Radiation,* **2005,** *12* (4), 537-541.

3. Wang, B.; Wang, L.; Mamoor, M.; Wang, C.; Zhai, Y.; Wang, F.; Jing, Z.; Qu, G.; Kong, Y.; Xu, L., Manipulating Atomic-Coupling in Dual-Cavity Boride Nanoreactor to Achieve Hierarchical Catalytic Engineering for Sulfur Cathode. *Angewandte Chemie International Edition,* **2024,** *63* (41), e202406065.

4. Zhang, W.; Pan, H.; Han, N.; Feng, S.; Zhang, X.; Guo, W.; Tan, P.; Xie, S.; Zhou, Z.; Ma, Q.; Guo, X.; Vlad, A.; Wübbenhorst, M.; Luo, J.; Fransaer, J., Balancing Adsorption, Catalysis, and Desorption in Cathode Catalyst For Li–S Batteries. *Advanced Energy Materials,* **2023,** *13* (43), 2301551.

5. Fei, B.; Zhang, C.; Cai, D.; Zheng, J.; Chen, Q.; Xie, Y.; Zhu, L.; Cabot, A.; Zhan, H., Hierarchical Nanoreactor with Multiple Adsorption and Catalytic Sites for Robust Lithium–Sulfur Batteries. *ACS Nano,* **2021,** *15* (4), 6849-6860.

6. Mu, J.; Jiang, H.; Yu, M.; Gu, S.; He, G.; Dai, Y.; Li, X., Thiophilic–Lithiophilic

Hierarchically Porous Membrane-Enabled Full Lithium–Sulfur Battery with a Low N/P Ratio. *ACS Applied Materials & Interfaces,* **2022,** *14* (20), 23408-23419.

7. Zhuang, H.; Zhang, T.; Xiao, H.; Zhang, F.; Han, P.; Gu, H.; Jiao, J.; Chen, W.; Gao, Q., Free-standing cross-linked hollow carbonaceous nanovesicle fibers with atomically dispersed CoN4 electrocatalytic centers driving high-performance Li-S battery. *Applied Catalysis B: Environmental,* **2024,** *340*.

8. Yan, M.; Wang, Z. Y.; Yu, G. W.; Huang, R.; Zhang, C. Y.; Chang, X. N.; Dong, W. D.; Liu, X. L.; Liu, J.; Mohamed, H. S. H.; Liu, Z. T.; Li, Y.; Su, B. L., Adsorption-Catalysis-Conversion of Polysulfides in Sandwiched Ultrathin $Ni(OH)_2$-PANI for Stable Lithium–Sulfur Batteries. *Small,* **2022,** *18* (25), 2201822.

9. Wang, B.; Wang, L.; Mamoor, M.; Wang, C.; Zhai, Y.; Wang, F.; Jing, Z.; Qu, G.; Kong, Y.; Xu, L., Manipulating Atomic-coupling in Dual-cavity Boride Nanoreactor to Achieve Hierarchical Catalytic Engineering for Sulfur Cathode. *Angewandte Chemie International Edition,* **2024**, e202406065.

10. Zhe, T.; Li, F.; Ma, K.; Liu, M.; Li, R.; Li, M.; Wang, C.; Luo, Q.; Lü, X.; Wang, L., Accelerated Oxygen Evolution Kinetics by Engineering Heterojunction Coupling of Amorphous NiFe Hydr(oxy)oxide Nanosheet Arrays on Self-Supporting Ni-MOFs. *Small,* **2023,** *19* (43), 2303303.